# Streaming Potential through Multilayer Membranes

**A. Szymczyk, C. Labbez, and P. Fievet**
Laboratoire de Chimie des Matériaux et Interfaces, 25030 Besançon cedex, France

**B. Aoubiza**
Laboratoire de Calcul Scientifique, 25030 Besançon cedex, France

**C. Simon**
Sintef Materials Technology, Blindem 0314 Oslo, Norway

*The fundamental and practical importance of electrokinetic characterization of porous membranes is now well recognized. However, not enough attention has focused on the fact that the most practically interesting membranes have a multilayer structure. Then, standard electrokinetic methods, such as streaming potential measurement performed through these multilayer membranes, lead to a global signal that does not necessarily reflect the electrokinetic behavior of the skin layer that rules the membrane selectivity. The relative influence of membrane layers with different physical (pore length, porosity, pore radius) and electrical (zeta potential) properties on the global streaming potential arising across a two-layer membrane is studied. Each porous layer plays a role in the streaming potential process, but in a wide range of length fraction of support layer the skin layer contributes more than the support layer to the global signal. The contribution of the skin layer increases as its porosity and pore radius decrease, but is little affected by its zeta potential. Nevertheless, in many practical situations, the support layer is likely to play a nonnegligible role on the global signal due to its huge thickness with respect to the skin layer. Therefore, electrokinetic measurements performed with multilayer membranes should be interpreted carefully.*

## Introduction

Most commercial filtration membranes are composite membranes made with two or more different layers, and each underlying layer has a progressively larger pore size and more important thickness. This asymmetric structure gives the membrane its required mechanical strength (which is provided by the support layer), along with its desired separation properties (which are governed by the skin layer).

It is now well recognized that separation properties of porous membranes do not depend only on their physical properties (including porosity and pore-size distribution) but also on their surface charge properties. All recent works dealing with membrane retention (Bacchin et al., 1996; Bowen and Mohammad, 1998; Combe et al., 1997; Hagmeyer and Gimbel, 1998; Levenstein et al., 1996; Nyström et al., 1998) or fouling phenomena (Causserand et al., 1997; Nyström et al., 1990, 1995) have underlined the role of surface interactions, which modify the transport of species that would be given by simple sieving effects.

From then on, understanding the electrokinetic mechanisms occurring during the filtration of solutions containing charged species appears to be a necessary step to predict the filtration efficiency of membranes. To this end, many studies have focused on the determination of membrane electrokinetic properties by standard electrokinetic methods such as streaming potential measurement (Ho et al., 1999; Nyström, 1989; Pontié, 1999; Szymczyk et al., 1998a; Thomas et al., 1987; Yan et al., 1993), which has proved to be a reliable way of determining the zeta potential of porous membranes. A major advantage of the streaming potential method is that it

Correspondence concerning this article should be addressed to A. Szymczyk.

allows the characterization of the membrane during the filtration process. The classical method consists in applying a pressure gradient through the membrane and measuring the resulting electrical potential difference arising on both sides of the membrane.

However, not enough attention has been paid to the investigation of the electrokinetic behavior of inhomogeneous porous media such as charged multilayer membranes. In such multilayer structures, each layer contributes to the global streaming potential measured across the membrane (Jin and Sharma, 1991). In a recent article, Szymcyzk et al. (1998b) have determined the skin layer electrokinetic properties of a multilayer ceramic membrane by coupling streaming potential and permeation flux measurements. It was shown that the global streaming potential measured across the multilayer membrane does not necessarily reflect the real properties of the skin layer, because of the nonnegligible pressure drop occurring across the thick support layer.

The present work is an attempt to evaluate the relative influence of physical (pore length, porosity, and pore size) and electrical (zeta potential) parameters on the global streaming potential arising across porous membranes consisting of two layers with different properties. It aims to point out that streaming potential measurements performed through multilayer membranes should be carefully interpreted, because the support layer of such membranes is likely to play a nonnegligible role in many practical cases.

## Theory

We consider a two-layer porous structure (see example described in Figure 1). Each layer ($k$) is considered to be a set of $N^{(k)}$ identical straight cylindrical pores of length $l^{(k)}$ and radius $a^{(k)}$ (with $l^{(k)} \gg a^{(k)}$) carrying an identical electrical charge. Layer 1 represents the support layer (that is, the layer with the largest pores) and layer 2 represents the skin layer. Each pore of the support layer is assumed to be connected in series with a given number or pores of the skin layer. We neglect interfacial phenomena that may occur at the junction between pores of both layers. The porosity of the support layer ($\epsilon^{(1)}$) is taken larger than (or equal to) that of the active layer ($\epsilon^{(2)}$). From these considerations, we can write

$$\frac{N^{(2)}}{N^{(1)}} = \frac{\epsilon^{(2)}}{\epsilon^{(1)}} \left( \frac{a^{(1)}}{a^{(2)}} \right)^2 \tag{1}$$

It is worth mentioning that if $a^{(1)} = a^{(2)}$, we set $N^{(1)} = N^{(2)}$ and so, $\epsilon^{(1)} = \epsilon^{(2)}$.

Let $X$, the length fraction of support layer, be defined as

$$X = \frac{l^{(1)}}{l^{(1)} + l^{(2)}} \tag{2}$$

We consider that the above-described membrane separates two electrolyte solutions at the same concentration and temperature, but different hydrostatic pressures and electrical potentials. We assume that neither the skin layer nor the support are selective to ions (that is, the electrolyte concentration is the same inside both layers). According to the linear theory of irreversible processes, the governing equations describing transport in a single pore of a layer $k$ (for sufficiently small transmembrane forces, that is, near the thermodynamic equilibrium) can be expressed as follows

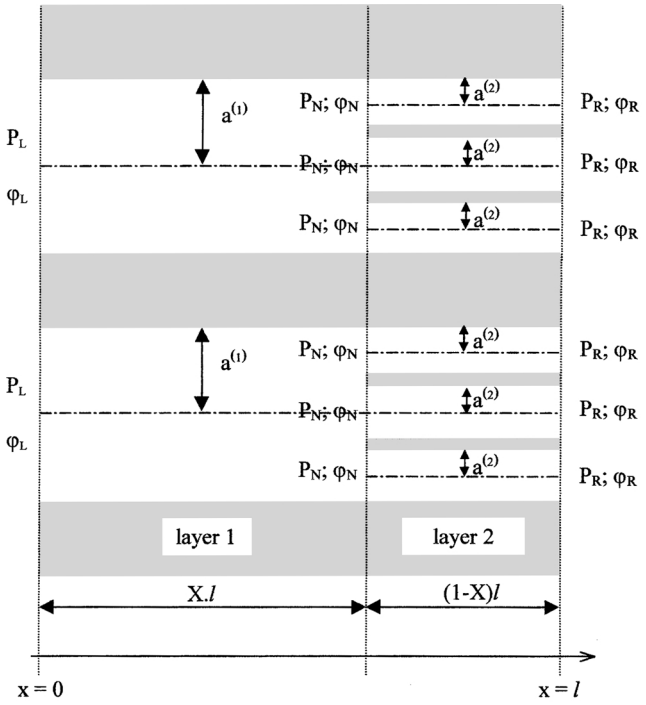


**Figure 1. Possible two-layer structure.**

$a^{(k)}$ is pore radius of layer $k$ ($k = 1$ for the support layer and $k = 2$ for the skin layer); $P$ is hydrostatic pressure; $\varphi$ is electrical potential; $l$ is membrane thickness; $X$ is length fraction of support layer.

$$q^{(k)} = K_{11}^{(k)} \left( \frac{\Delta P^{(k)}}{l^{(k)}} \right) + K_{12}^{(k)} \left( \frac{\Delta \varphi^{(k)}}{l^{(k)}} \right) \tag{3a}$$

$$I^{(k)} = K_{21}^{(k)} \left( \frac{\Delta P^{(k)}}{l^{(k)}} \right) + K_{22}^{(k)} \left( \frac{\Delta \varphi^{(k)}}{l^{(k)}} \right) \tag{3b}$$

where $q^{(k)}$ and $I^{(k)}$ are the solvent flow and the electrical current, respectively, and $\Delta P^{(k)}$ and $\Delta \varphi^{(k)}$ are the hydrostatic pressure and the electrical potential differences between pore ends, respectively. $K_{ij}^{(k)}$ are the so-called phenomenological coefficients coupling flows and forces. The matrix of these coefficients is symmetric, that is, $K_{ij}^{(k)} = K_{ji}^{(k)}$ (Onsager's theorem). Calculations presented in this work are carried out using the expressions of phenomenological coefficients listed in the Appendix. The establishment of these integral expressions has been described elsewhere (Syzmczyk et al., 1999) in the framework of a classical space charge model as outlined by Osterle and coworkers (Fair and Osterle, 1971; Gross and Osterle, 1968; Morrison and Osterle, 1965).

According to Figure 1, the following boundary conditions are set

$$P_{(x=0)} = P_L \tag{4a}$$

$$\varphi_{(x=0)} = \varphi_L \tag{4b}$$

$$P_{(x=l)} = P_R \tag{4c}$$

$$\varphi_{(x=l)} = \varphi_R \tag{4d}$$

We define the global streaming potential ($SP_g$) as the ratio of the electrical potential drop ($\Delta\varphi = \varphi_L - \varphi_R$) to the hydrostatic pressure drop ($\Delta P = P_L - P_R$) across the two-layer structure under zero electrical current conditions

$$SP_g = \left(\frac{\Delta\varphi}{\Delta P}\right)_{I=0} \tag{5}$$

Taking into account Eqs. 1–3 and applying conservation law for solvent flow and electrical current across the membrane leads to the following expression for global streaming potential

$$SP_g = \frac{\left[-(1-X)\left(K_{12}^{(1)}K_{21}^{(1)} - K_{11}^{(1)}K_{22}^{(1)}\right) - \frac{N^{(2)}}{N^{(1)}}XK_{21}^{(1)}K_{12}^{(2)}\right]K_{21}^{(2)} + \frac{N^{(2)}}{N^{(1)}}XK_{21}^{(1)}K_{11}^{(2)}K_{22}^{(2)}}{\frac{N^{(2)}}{N^{(1)}}XK_{22}^{(1)}K_{12}^{(2)}K_{21}^{(2)} - \left[-(1-X)\left(K_{12}^{(1)}K_{21}^{(1)} - K_{11}^{(1)}K_{22}^{(1)}\right) + \frac{N^{(2)}}{N^{(1)}}XK_{22}^{(1)}K_{11}^{(2)}\right]K_{22}^{(2)}} \tag{6}$$

When $X = 1$, Eq. 6 reduces to

$$SP^{(1)} = -\frac{K_{21}^{(1)}}{K_{22}^{(1)}} \tag{7}$$

where $SP^{(1)}$ represents the streaming potential across layer 1. The above equation is concurrent with the expression of streaming potential in the formalism of the thermodynamics of irreversible processes for a single pore.

Similarly, the streaming potential across layer 2 ($SP^{(2)}$) is obtained from Eq. 6 by setting $X = 0$

$$SP^{(2)} = -\frac{K_{21}^{(2)}}{K_{22}^{(2)}} \tag{8}$$

Dividing both numerator and denominator of Eq. 6 by $XK_{22}^{(2)}K_{22}^{(1)}$, considering Eqs. 1, 7, and 8 and rearranging yields

$$SP_g = \frac{XSP^{(1)} + SP^{(2)}\left(\frac{a^{(1)}}{a^{(2)}}\right)^2(1-X)\frac{\epsilon^{(1)}}{\epsilon^{(2)}}\frac{F^{(2)}}{F^{(1)}}}{X + \left(\frac{a^{(1)}}{a^{(2)}}\right)^2(1-X)\frac{\epsilon^{(1)}}{\epsilon^{(2)}}\frac{F^{(2)}}{F^{(1)}}} \tag{9}$$

with $F^{(k)}$ ($k = 1$ or 2)

$$F^{(k)} = \frac{1}{1 - \frac{K_{12}^{(k)}K_{21}^{(k)}}{K_{11}^{(k)}K_{22}^{(k)}}} \tag{10}$$

$F^{(k)}$ describes electroviscous effects inside pores of layer $k$ (that is, the increase in apparent viscosity of the fluid resulting from the presence of electrical double layers inside pores (Hunter, 1981)) and can be viewed as the ratio of the Poiseuille flow (the fluid flow in the absence of double layer effects, that is, at the isoelectric point or at high electrolyte concentration) to the observed fluid flow.

The hydraulic permeability of a layer ($Lp^{(k)}$), made with $N^{(k)}$ identical pores of radius $a^{(k)}$ and length $l^{(k)}$, can be expressed as follows

$$Lp^{(k)} = \frac{\pi N^{(k)}a^{(k)4}}{8\mu l^{(k)}F^{(k)}} \tag{11}$$

where $\mu$ is the fluid viscosity.

Considering Eqs. 1, 2, and 11, we can write for a two-layer membrane

$$\frac{Lp^{(1)}}{Lp^{(2)}} = \left(\frac{a^{(1)}}{a^{(2)}}\right)^2\frac{(1-X)}{X}\frac{\epsilon^{(1)}}{\epsilon^{(2)}}\frac{F^{(2)}}{F^{(1)}} \tag{12}$$

Substituting the above relation into Eq. 9 gives

$$SP_g = \frac{SP^{(1)} + SP^{(2)}\frac{Lp^{(1)}}{Lp^{(2)}}}{1 + \frac{Lp^{(1)}}{Lp^{(2)}}} \tag{13}$$

## Materials and Methods

### *Chemicals*

Electrolyte solutions are prepared from potassium chloride of pure analytical grade and milli-Q quality water. The pH of solutions is that of milli-Q water, being $5.60 \pm 0.05$. The whole experimental study is carried out at $25 \pm 0.5$°C.

### *Membranes*

The porous media used in this work are noncommercial alumina membranes produced by Sintef Materials and Technology (Oslo, Norway) in the form of 47 mm diameter discs. Three different structures are studied (see characteristics in Table 1): two monolayer membranes having different pore sizes (the membrane with larger pores plays the role of the support layer, and the membrane with smaller pores plays the role of the skin layer) and a two-layer membrane made with support and skin layer.

**Table 1. Physical Characteristics of Monolayer Alumina Membranes***

| | Support Layer | Skin Layer |
|---|---|---|
| Mean pore radius | 200 nm | 60 nm |
| Porosity | 26% | 20% |
| Thickness | 1 mm | 1 mm |

*Noncommercial membranes produced by Sintef Materials Technology (Oslo, Norway). The two-layer membrane consists of support and skin layer with $X = 0.980$.

### *Streaming potential measurements*

The device employed for streaming potential measurements is similar to that previously described (Szymczyk et al., 1998a). The membrane is soaked overnight in the electrolyte solution under consideration; then, the solution is forced through the membrane under a transmembrane pressure of 1 bar for about 8 h to equilibrate the membrane with the solution. During the experiment, both compartments separated by the membrane are filled with the feed solution, which is continuously recycled. The conductivity of the solution on each side of the membrane is regularly checked. At a given time, a pressure pulse of 1 bar is applied on one side of the membrane. The instantaneous resulting electrical potential difference is measured by means of Ag/AgCl electrodes and a high impedance milli-voltmeter. This electrical potential difference is recorded so as to determine the streaming potential value. All experiments are repeated three times. Pressure and electrical potential differences are measured at $\pm 0.01$ bar and $\pm 0.1$ mV, respectively.

## Results and Discussion

Numerical calculations presented in this work have been carried out for a range of porosities, pore sizes and zeta potentials that may commonly occur in experimental investigations with filtration membranes. The electrolytic medium considered in the strictly theoretical part of the study is a 0.001 M potassium chloride solution at a temperature $T$ of 298 K.

Let us consider the function $Y$ defined as follows

$$Y = \frac{SP_g - SP^{(1)}}{SP^{(2)} - SP^{(1)}} \tag{14}$$

The function $Y$ therefore represents the relative contribution of the skin layer (layer 2) to the global streaming potential ($SP_g$). It has the advantage that its range is bounded between 0 (for $SP_g = SP^{(1)}$) and 1 (for $SP_g = SP^{(2)}$), while $SP_g$ ranges from $SP^{(1)}$ to $SP^{(2)}$. Substituting Eq. 13 into Eq. 14, $Y$ can be rewritten as follows

$$Y = \frac{\dfrac{Lp^{(1)}}{Lp^{(2)}}}{1 + \dfrac{Lp^{(1)}}{Lp^{(2)}}} \tag{15}$$

Thus, the relative contribution of the skin layer to the global electrical signal depends on the hydraulic permeability ratio between both layers, as exposed in Figure 2. Since the permeation flux is identical through both layers (conservation law), the hydraulic permeability ratio can be expressed as

$$\frac{Lp^{(1)}}{Lp^{(2)}} = \frac{\Delta P^{(2)}}{\Delta P^{(1)}} \tag{16}$$

where $\Delta P^{(1)}$ and $\Delta P^{(2)}$ are the pressure drops across support and skin layer, respectively.

Then, the greater the pressure drop (that is, the driving force that gives rise to the streaming potential phenomenon) across a porous layer, the more this layer will contribute to the electrical signal measured through the whole membrane.

According to Eq. 12, the hydraulic permeability ratio depends on physical and electrical parameters, namely the porosity ratio, the pore length fraction, the pore radius ratio, and the electroviscous effect ratio. Let us now discuss the

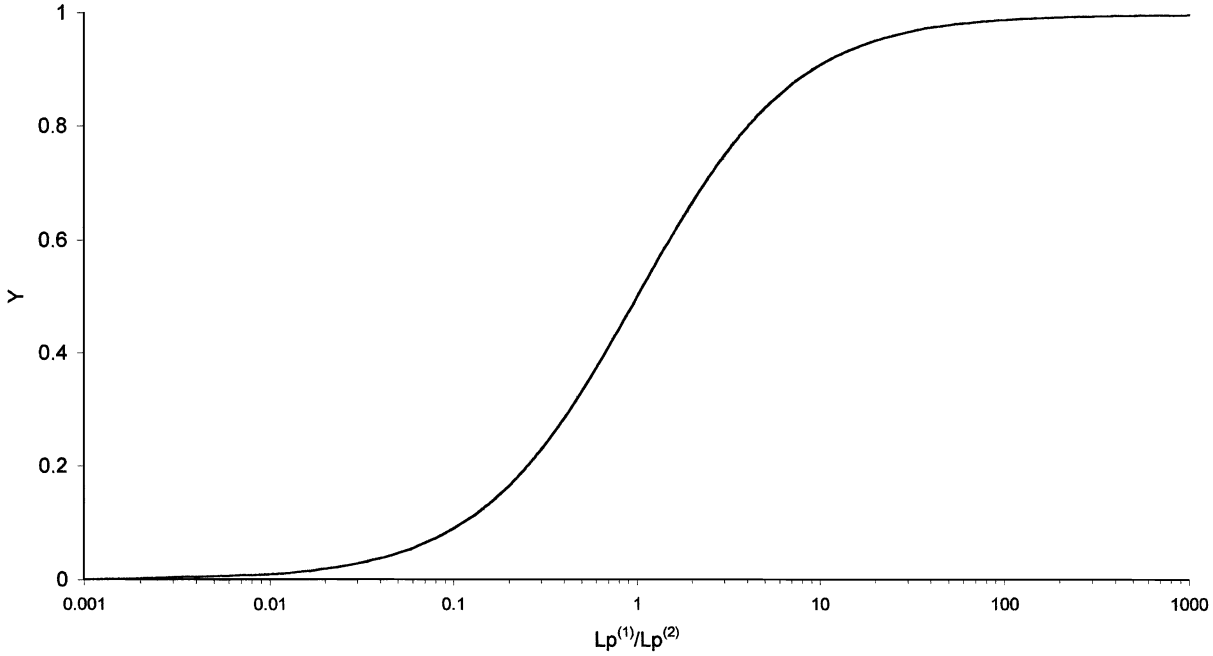


**Figure 2. Variation of the relative contribution (Y) of the skin layer to the global streaming potential vs. hydraulic permeability ratio of both layers ($Lp^{(1)}/Lp^{(2)}$).**

influence of these parameters in terms of relative contribution of the skin layer to the global streaming potential.

Figure 3 shows the variation of $Y$ vs. length fraction of the support layer ($X$) for various porosity ratios ($\epsilon^{(1)}/\epsilon^{(2)}$) ranging from 1 to 3. The system is assumed to be a composite membrane consisting of two distinct layers with pores that are 100 and 50 nm in radius and identically charged ($\zeta^{(1)} = \zeta^{(2)} = 50$ mV). As can be seen, smaller pores have a stronger influence on the global electrical signal than larger ones (an identical effect of both kinds of pores would lead to a linear variation of $Y$ vs. $X$). This is not unexpected since the pressure drop across the skin layer is likely to be greater than the pressure drop across the support layer for a wide range of $X$. The influence of smaller pores increases as the porosity ratio ranges from 1 to 3. Indeed, the hydraulic resistance of the skin layer becomes greater as its porosity ($\epsilon^{(2)}$) decreases with respect to that of the support layer. As a result, the pressure drop across the skin layer increases, which leads to a greater contribution of this layer to the global streaming potential.

Figure 4 shows the variation of $Y$ vs. length fraction of the support layer ($X$) for various values of $\zeta^{(1)}$ and $\zeta^{(2)}$. The system considered here is a two-layer membrane made with pores that are equal in radius ($a^{(1)} = a^{(2)} = 10$ nm), but carrying a different electrical charge ($\zeta^{(1)} \neq \zeta^{(2)}$). Pores are assumed to be connected end-to-end so that $\epsilon^{(1)}/\epsilon^{(2)} = 1$.

First, it is interesting to note that a porous layer influences the global electrical signal even if its pores carry no electrical charge ($\zeta = 0$). Indeed, there is a pressure drop across the porous layer even if this latter is uncharged and then, this layer contributes to the global streaming potential.

It also appears in Figure 4 that the variation of zeta potentials play only a minor role on $Y$ at a fixed pore length fraction. Considering Eqs. 12 and 15, it appears that zeta potential affects the function $Y$ only by means of the electroviscous effect ratio ($F^{(2)}/F^{(1)}$). An example of zeta potential dependence of electroviscous effects is shown in Figure 5, where $F^{(k)}$ is plotted vs. $\zeta^{(k)}$ for a single pore $k$ of 10 nm in radius. It appears in this example that the range of $F^{(k)}$ is bounded between 1 and $\sim 1.25$. Literature (Bowen and Jenner, 1995; Szymczyk et al., 1999) shows that electroviscous effects occurring inside a porous medium do not exceed the value of about 1.5, whatever the electrolyte, the pore size, or the electrical charge carried by the pore walls. The ratio $F^{(2)}/F^{(1)}$ is therefore close to 1, which explains the small influence of $\zeta^{(1)}$ and $\zeta^{(2)}$ on the relative contribution of layer 2 to the global streaming potential, as can be seen in Figure 4.

Figure 6 shows the variation of $Y$ vs. $X$ for various pore radius ratios ranging from 2 to 10. The zeta potentials of both kinds of pores are taken identical, and the porosity ratio is fixed at a value of 2. It appears that the higher the pore-size ratio, the more the skin layer contributes to the global signal (at fixed length fraction and porosity ratio). For example, it can be seen for $a^{(1)}/a^{(2)} = 10$ that the streaming potential across the whole membrane is almost the same as that of the skin layer for $X$ ranging from 0 to about 0.9. Nevertheless, it is essential to keep in mind that, for commercial membranes, $X$ is usually higher than 0.98 (the support layer is very thick to provide the necessary mechanical strength whereas the skin layer is very thin to allow high permeation fluxes). As can be seen in Figure 6, the contribution of the skin layer dramatically falls within this region of $X$ and, then, streaming potential measured through a multilayer membrane may not reflect the electrokinetic behavior of the skin layer. Hence, care must be taken to interpret electrokinetic data for multilayer membranes.

It should be noted that results presented in Figure 6 do not take into account the variation of pore radius ratio only, but also the variation of $F^{(2)}/F^{(1)}$, since electroviscous effects

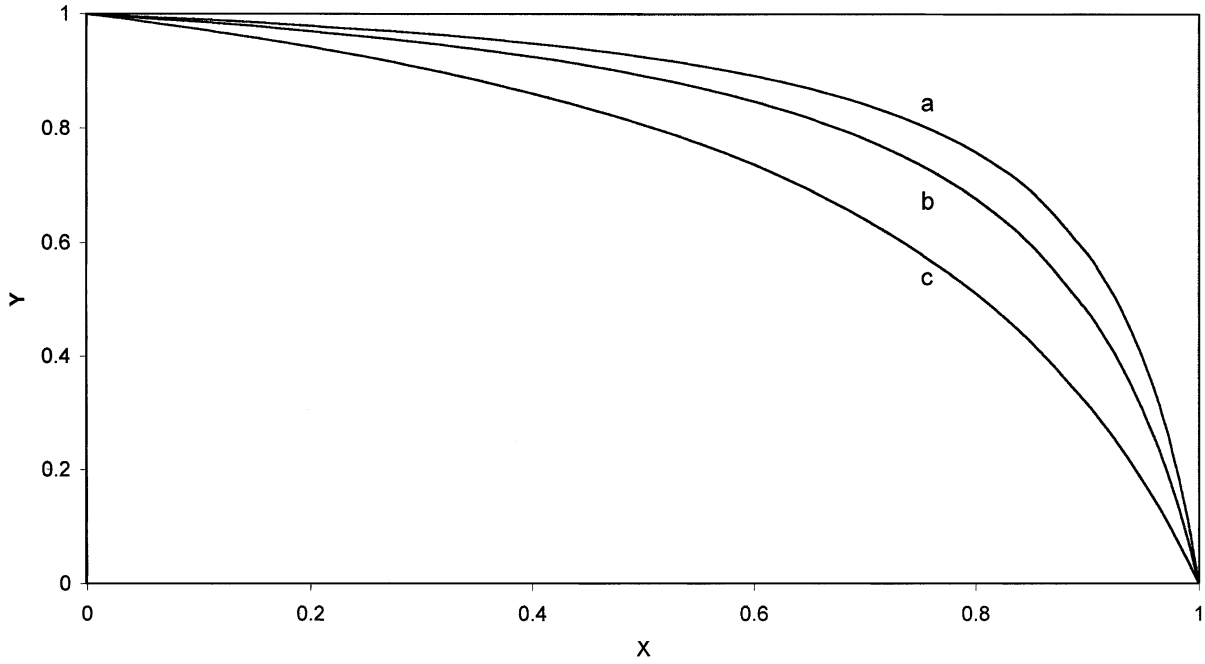


**Figure 3. Variation of Y vs. length fraction of support layer (X) for various porosity ratios.**

($\epsilon^{(1)}/\epsilon^{(2)}$); $a^{(1)} = 100$ nm; $a^{(2)} = 50$ nm; $\zeta^{(1)} = \zeta^{(2)} = 50$ mV; 0.001 mol·L$^{-1}$ KCl; T = 298 K. a: $\epsilon^{(1)}/\epsilon^{(2)} = 3$; b: $\epsilon^{(1)}/\epsilon^{(2)} = 2$; c: $\epsilon^{(1)}/\epsilon^{(2)} = 1$.

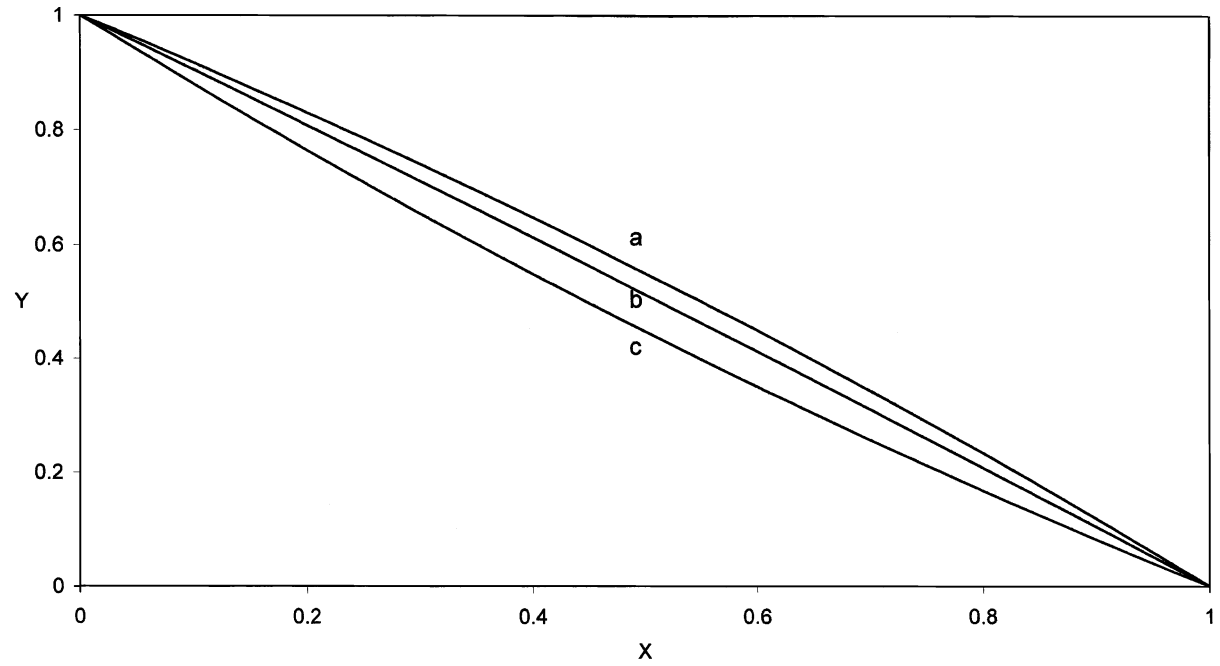


**Figure 4. Variation of *Y* vs. *X* for various couples of zeta potential.**

$a^{(1)} = a^{(2)} = 10$ nm; $\epsilon^{(1)}/\epsilon^{(2)} = 1$; 0.001 mol·L$^{-1}$ KCl; T = 298 K. a: $\zeta^{(1)} = 0$ mV, $\zeta^{(2)} = 150$ mV; b: $\zeta^{(1)} = 0$ mV, $\zeta^{(2)} = 50$ mV; c: $\zeta^{(1)} = 150$ mV, $\zeta^{(2)} = 0$ mV.

depend on pore size at fixed zeta potential (Szymczyk et al., 1999). However, as previously mentioned, the ratio $F^{(2)}/F^{(1)}$ is always close to 1 and, then electroviscous effects play a negligible role with respect to pore radius ratio that is squared in Eq. 12.

Experimental results are presented in Figure 7 where streaming potentials of three different membranes (two monolayer membranes that play the role of support and skin layer, and a two-layer membrane made with support and skin layer) are plotted vs. concentration of potassium chloride so-

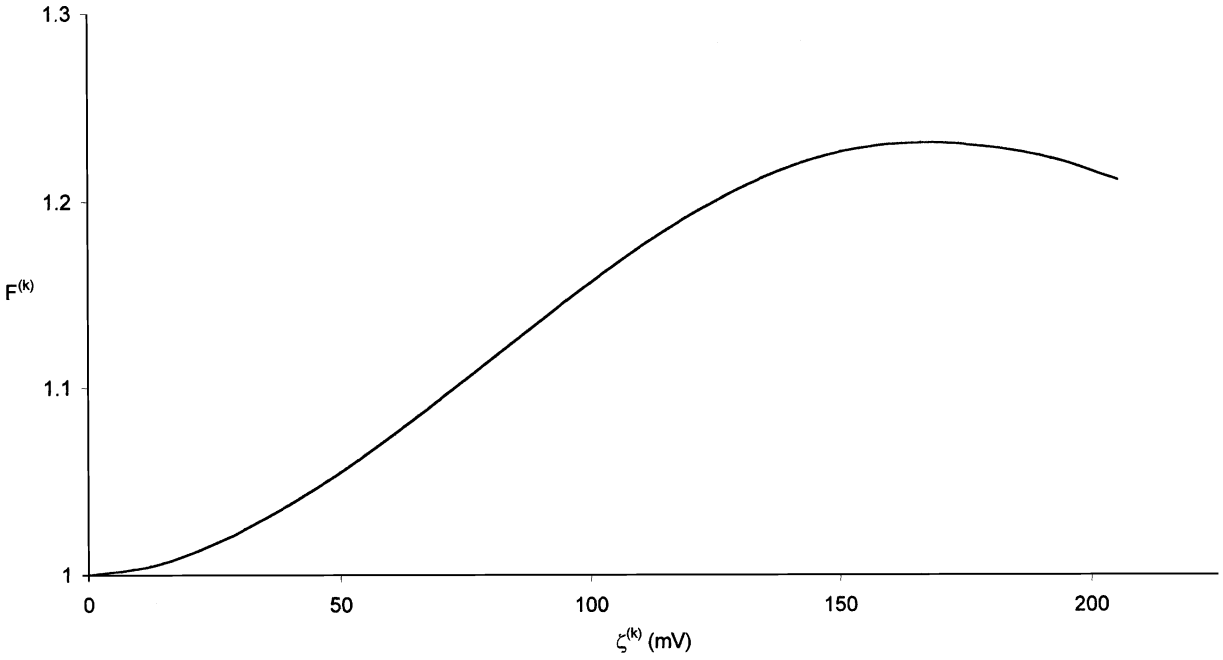


**Figure 5. Zeta potential ($\zeta^{(k)}$) dependence of $F^{(k)}$.**

$a^{(k)} = 10$ nm; 0.001 mol·L$^{-1}$ KCl; T = 298 K.

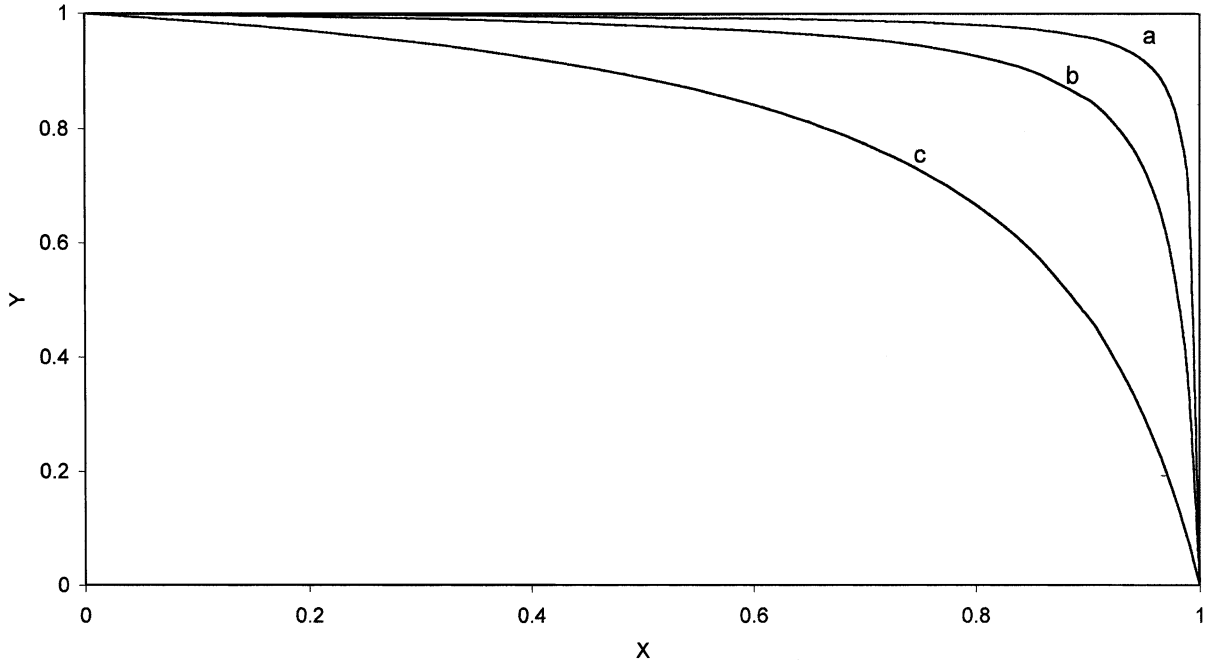


**Figure 6. Variation of *Y* vs. length fraction of support layer (*X*) for various pore radius ratios.**

$(a^{(1)}/a^{(2)})$; $\zeta^{(1)} = \zeta^{(2)} = 50$ mV; $\epsilon^{(1)}/\epsilon^{(2)} = 2$; 0.001 mol·L$^{-1}$; KCl; T = 298 K. a: $a^{(1)} = 500$ nm, $a^{(2)} = 50$ nm; b: $a^{(1)} = 500$ nm, $a^{(2)} = 100$ nm; c: $a^{(1)} = 500$ nm, $a^{(2)} = 250$ nm.

lutions. The global streaming potential computed from the component membrane layers is also plotted. A very good agreement between experimental and theoretical global streaming potential is observed since discrepancies do not exceed about 6%. The simple approach, considering both layers as being connected in series, therefore seems to provide quite a good description of electrokinetic phenomena occurring through a composite membrane. As expected, for all membranes, streaming potential decreases as ionic strength increases due to the so-called double layer compression phe-

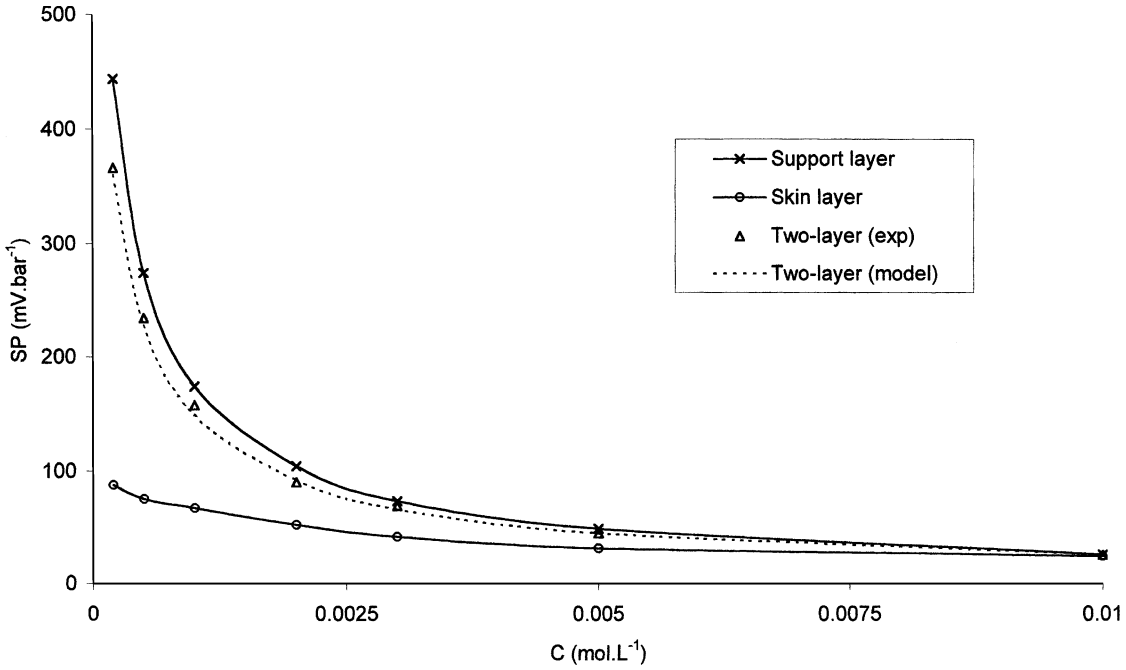


**Figure 7. Experimental and theoretical streaming potentials (*SP*) of various alumina membranes vs. electrolyte concentration (*C*).**

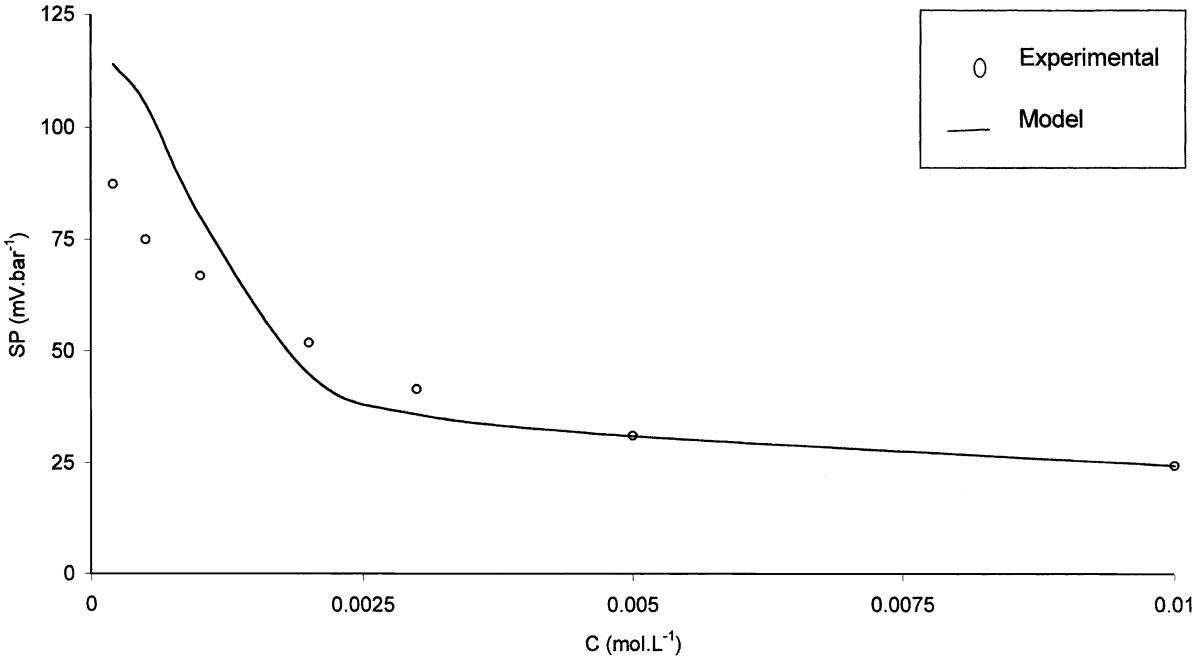


**Figure 8. Experimental and theoretical streaming potential of the skin layer vs. electrolyte concentration ($C$).**

nomenon (Hunter, 1996). The global streaming potential measured through the two-layer membrane is close to that of the support layer; that is to say that the skin layer hardly affects the electrokinetic behavior of the two-layer membrane. Similar observations have already been reported by Szymczyk et al. (1998b) in a work dealing with electrokinetic characterization of multilayer ceramic membranes. In the present case, the weak contribution of the skin layer is mainly due to the small pore radius and porosity ratios ($a^{(1)}/a^{(2)} = \sim 3.3$; $\epsilon^{(1)}/\epsilon^{(2)} = 1.3$) whereas the support layer represents roughly 98% of the membrane thickness. Of course, in the case of commercial membranes, the skin layer is expected to play a greater role because large pore-size ratios are usually encountered. Nevertheless, it must be kept in mind that the support layer is likely to play a nonnegligible role in many practical cases due to its huge thickness with respect to the skin layer (this is particularly true for ceramic membranes).

Figure 8 shows the comparison between the experimental and theoretical streaming potential of the skin layer vs. electrolyte concentration. A rather good agreement is obtained, but discrepancies between experiment and calculation are more pronounced (up to about 30% in the worst case) than for the global streaming potential of the composite membrane. This is due to the form of Eq. 13. In the case of the composite membrane under consideration, the ratio $Lp^{(1)}/Lp^{(2)}$ is close to 0.3, that is to say that the hydraulic resistance of the skin layer is over 3 times smaller than that of the support layer. In such a case, a small variation of $Lp^{(1)}/Lp^{(2)}$ leads to a significant variation of the skin layer streaming potential. On the other hand, if $Lp^{(1)}/Lp^{(2)}$ is $\gg 1$, a small variation of $Lp^{(1)}/Lp^{(2)}$ leads to a negligible variation of the skin layer streaming potential. Consequently, a better agreement between theoretical and experimental results would be expected using commercial composite membranes for which the hydraulic resistance of the skin layer usually exceeds that of the support layer. Unfortunately, no experiment could be carried out with commercial membranes since no autosupported skin layer is currently available separately.

## Conclusion

Streaming potential measured across composite porous membranes has been investigated using the simple approach of porous layers connected in series. A relation between the global streaming potential of a two-layer membrane and the individual streaming potentials of support and skin layer has been established. This relation involves pore length, porosity and pore radius of support and skin layers, as well as their zeta potential (which affects electroviscous effects occurring within pores). The comparison between experimental and theoretical results gives quite good agreements. The global streaming potential is intermediate between individual signals of both layers, but the contribution of the skin layer is greater than that of the support layer in a wide range of length fraction of the support layer. This contribution is little influenced by zeta potential and increases as porosity and pore radius of the skin layer decrease (that is, when the hydraulic resistance of the skin layer increases with respect to that of the support layer). Nevertheless, since the support layer overwhelmingly dominates the membrane thickness in most practical situations, the contribution of the support layer to the global electrical signal may be more or less important. Streaming potential measurements performed through multilayer membranes should then be carefully interpreted.

## Notation

$a^{(k)}$ = pore radius of layer $k$, m
$C$ = bulk electrolyte concentration, mol·m$^{-3}$
$c_n^{(k)}$ = concentration of ions $n$ inside pores of layer $k$, mol·m$^{-3}$
$F$ = Faraday constant ( = 96 485 C·mol$^{-1}$)
$F^{(k)}$ = electroviscous effects in layer $k$

$I^{(k)}$ = electrical current across pores of layer $k$, A
$K_n$ = Mobility of ions $n$, $m \cdot s^{-1} \cdot N^{-1} \cdot mol$
$K_{ij}^{(k)}$ = phenomenological coefficients for pores of layer $k$
$l$ = thickness of the two-layer membrane, m
$l^{(k)}$ = thickness of layer $k$, m
$N^{(k)}$ = pore number in layer $k$
$P$ = hydrostatic pressure, $N \cdot m^{-2}$
$q^{(k)}$ = solvent flow through a pore of layer $k$, $m^3 \cdot s^{-1}$
$r$ = radial coordinate, m
$R$ = universal gas constant, 8.314 $J \cdot mol^{-1} \cdot K^{-1}$
$SP^{(k)}$ = streaming potential through layer, $k$ $V \cdot N^{-1} \cdot m^2$
$SP_g$ = global streaming potential through two-layer membrane, $V \cdot N^{-1} \cdot m^2$
$T$ = temperature, K
$x$ = axial coordinate, m
$X$ = length fraction of support layer
$Y$ = relative contribution of the skin layer to the global streaming potential
$z_n$ = charge number of the ionic species $n$
$z$ = absolute value of $z_n$

### *Greek letters*

$\epsilon_0$ = vacuum permittivity, $8.854 \times 10^{-12}$ $F \cdot m^{-1}$
$\epsilon_r$ = relative dielectric constant of the solvent, 79.8
$\epsilon^{(k)}$ = porosity of layer $k$
$\mu$ = viscosity of the electrolyte, 0.001 $kg \cdot m^{-1} \cdot s^{-1}$
$\pi$ = standard dimensionless constant
$\varphi$ = electrical potential, V
$\psi^{(k)}$ = electrostatic potential inside pores of layer $k$, V
$\zeta^{(k)}$ = zeta potential of layer $k$, V

## Literature Cited


Bacchin, P., P. Aimar, and V. Sanchez, "Influence of Surface Interaction on Transfer During Colloid Ultrafiltration," *J. Memb. Sci.*, **115**, 49 (1996).

Bowen, W. R., and F. Jenner, "Electroviscous Effects in Charged Capillaries," *J. Colloid Int. Sci.*, **173**, 388 (1995).

Bowen, W. R., and A. W. Mohammad, "A Theoretical Basis for Specifying Nanofiltration Membranes-Dye/Salt/Water Streams," *Desalination*, **117**, 257 (1998).

Causserand, C., K. Jover, P. Aimar, and M. Meireles, "Modification of Clay Cake Permeability by Adsorption of Protein," *J. Memb. Sci.*, **137**, 31 (1997).

Combe, C., C. Guizard, P. Aimar, and V. Sanchez, "Experimental Determination of Four Characteristics Used to Predict the Retention of a Ceramic Nanofiltration Membrane," *J. Memb. Sci.*, **129**, 147 (1997).

Fair, J. C., and J. F. Osterle, "Reverse Electrodialysis in Charged Capillary Membranes," *J. Chem. Phys.*, **54**, 3307 (1971).

Gross, R. J., and J. F. Osterle, "Membrane Transport Characteristics of Ultrafine Capillaries," *J. Chem. Phys.*, **54**, 228 (1968).

Hagmeyer, G., and R. Gimbel, "Modelling the Salt Rejection of Nanofiltration Membranes for Ternary Ion Mixtures and for Single Salts at Different pH Values," *Desalination*, **117**, 247 (1998).

Ho, A. K., J. M. Perera, D. E. Dunstan, G. W. Stevens, and M. Nyström, "Measurement and Theoretical Modeling of Protein Mobility Through Membranes," *AIChE J.*, **45**, 1434 (1999).

Hunter, R. J., *Zeta Potential in Colloid Science. Principles and Applications*, Academic Press, London (1981).

Hunter, R. J., *Introduction to Modern Colloid Science*, Oxford Science Publications, New York (1996).

Jin, M., and M. Sharma, "A Model for Electrochemical and Electrokinetic Coupling Inhomogeneous Porous Media," *J. Coll. Interf. Sci.*, **141**, 61 (1991).

Levenstein, R., D. Hasson, and R. Semiat, "Utilization of the Donnan Effect for Improving Electrolyte Separation with Nanofiltration Membranes," *J. Memb. Sci.*, **116**, 77 (1996).

Morrison, F. A., and J. F. Osterle, "Electrokinetic Energy Conversion in Ultrafine Capillaries," *J. Chem. Phys.*, **43**, 2111 (1965).

Nyström, M., "Fouling of Unmodified Polysulfone UF Membranes by Ovalbumine," *J. Memb. Sci.*, **44**, 183 (1989).

Nyström, M., M. Laatikanien, K. Turku, and P. Järvinen, "Resistance to Fouling Accomplished by Modification of Ultrafiltration Membranes," *Prog. Colloid Poly. Sci.*, **82**, 321 (1990).

Nyström, M., L. Kaipia, and S. Luque, "Fouling and Retention of Nanofiltration Membranes," *J. Memb. Sci.*, **98**, 249 (1995).

Nyström, M., P. Aimar, S. Luque, M. Kulovaara, and S. Metsämuuronen, "Fractionation of Model Proteins Using their Physiochemical Properties," *Colloids and Surfaces A.*, **138**, 185 (1998).

Pontié, M., "Effect of Aging on UF Membranes by a Streaming Potential (SP) Method," *J. Memb. Sci.*, **154**, 213 (1999).

Szymczyk, A., P. Fievet, M. Mullet, J. C. Reggiani, and J. Pagetti, "Comparison of Two Electrokinetic Methods Electro-osmosis and Streaming Potential to Determine the Zeta-Potential of Plane Ceramic Membranes," *J. Memb. Sci.*, **143**, 293 (1998a).

Szymcyzk, A., P. Fievet, J. C. Reggiani, and J. Pagetti, "Determination of the Filtering Layer Electrokinetic Properties of a Multi-Layer Ceramic Membrane," *Desalinaiton*, **116**, 81 (1998b).

Szymczyk, A., B. Aoubiza, P. Fievet, and J. Pagetti, "Electrokinetic Phenomena in Homogeneous Cylindrical Pores," *J. Colloid Interface Sci.*, **216**, 285 (1999).

Thomas, K. C., V. Ramachandhran, and B. M. Misra, "Electrochemical and Electrokinetic Characterization of Cellulose Acetate Polymeric Membranes," *J. Appl. Poly. Sci.*, **34**, 2527 (1987).

Yan, F., P. Déjardin, and A. Schmidt, "Electrochemical Characterization of a Hemodialysis Membrane," *J. Phys. Chem.*, **97**, 3824 (1993).


## Appendix

The integral expressions of phenomenological coefficients that are used to compute global streaming potential are as follows

$$K_{11}^{(k)} = \frac{\pi a^{(k)^4}}{8\mu} \tag{17a}$$

$$K_{12}^{(k)} = \frac{2\pi zF}{\mu} \int_0^{a^{(k)}} r \int_r^{a^{(k)}} \frac{1}{r} \int_0^r \left(c_c^{(k)} - c_a^{(k)}\right) r \, dr dr dr \tag{17b}$$

$$K_{21}^{(k)} = K_{12}^{(k)} \tag{17c}$$

$$K_{22}^{(k)} = 2\pi z^2 F^2 \int_0^{a^{(k)}} \left(K_c c_c^{(k)} + K_a c_a^{(k)}\right) r dr + \frac{2\pi z^2 F^2}{\mu} \int_0^{a^{(k)}} r \left(c_c^{(k)} - c_a^{(k)}\right) \int_r^{a^{(k)}} \frac{1}{r} \int_0^r \left(c_c^{(k)} - c_a^{(k)}\right) r \, dr dr dr \tag{17d}$$

The local concentrations of cations and anions within pores of a layer $k$ ($c_c^{(k)}$ and $c_a^{(k)}$, respectively) are given by the Boltzmann equation

$$c_n^{(k)} = C \exp\left(\frac{z_n F \Psi^{(k)}}{RT}\right) \qquad n = a \,(\text{anion}) \text{ or } c \,(\text{cation}) \tag{18}$$

where $\Psi^{(k)}$ (electrostatic potential inside pores of layer $k$) is the solution of the Poisson-Boltzmann equation

$$\frac{\epsilon_0 \epsilon_r RT}{2C(zF)^2} r^{-1} \left\{ \frac{\partial}{\partial r} \left[ r \frac{\partial}{\partial r} \left( \frac{zF\Psi^{(k)}}{RT} \right) \right] \right\} = \sinh\left( \frac{zF\Psi^{(k)}}{RT} \right) \quad (19)$$

with the following boundary conditions

$$\Psi^{(k)}|_{r=a^{(k)}} = \zeta^{(k)} \quad (20)$$

and

$$\left. \frac{d\Psi^{(k)}}{dr} \right|_{r=0} = 0. \quad (21)$$

*Manuscript received Feb. 28, 2001.*